

# Predictions for $p + \text{Pb}$ at 5.02A TeV to test initial state nuclear shadowing at the Large Hadron Collider.

G. G. Barnaföldi,<sup>1</sup> J. Barrette,<sup>2</sup> M. Gyulassy,<sup>3,1</sup>  
P. Levai,<sup>1</sup> G. Papp,<sup>4</sup> M. Petrovici,<sup>5</sup> and V. Topor Pop<sup>2</sup>

<sup>1</sup>*WIGNER RCP, Institute for Particle and Nuclear  
Physics P.O.Box 49, Budapest, 1525, Hungary*

<sup>2</sup>*McGill University, Montreal, H3A 2T8, Canada*

<sup>3</sup>*Columbia University, New York, N.Y. 10027, USA*

<sup>4</sup>*Eötvös Loránd University, Pázmány Péter Sétány 1/A, H-1117 Budapest, Hungary*

<sup>5</sup>*National Institute for Physics and Nuclear  
Engineering- Horia Hulubei, R-077125, Bucharest, Romania*

(Dated: December 11, 2012)

## Abstract

Collinear factorized perturbative quantum chromodynamics (pQCD) model predictions are compared for  $p + \text{Pb}$  at 5.02A TeV to test nuclear shadowing of parton distribution at the Large Hadron Collider (LHC). The pseudorapidity distribution the nuclear modification factor (NMF),  $R_{p\text{Pb}}(y = 0, p_T < 20 \text{ GeV}/c) = dn_{p\text{Pb}}/(N_{\text{coll}}(b)dn_{pp})$  and the pseudorapidity asymmetry  $Y_{\text{asym}}^h(p_T) = R_{p\text{Pb}}^h(p_T, \eta < 0)/R_{p\text{Pb}}^h(p_T, \eta > 0)$  are computed using HIJING/B $\bar{\text{B}}$  v2.0 model and a pQCD improved parton model kTpQCD\_v2.0 which embedded generalized parton distribution functions (PDFs). These results are updated calculations of those presented in Ref. [1].

PACS numbers: 12.38.Mh, 24.85.+p, 25.75.-q, 24.10Lx

## I. INTRODUCTION

In this note we show predictions for moderate  $p_T < 20$  GeV/ $c$  observables in  $p + \text{Pb}$  collisions at 5.02A TeV at the Large Hadron Collider (LHC) using the HIJING/B $\bar{\text{B}}$  v2.0 model [1–3] and a pQCD improved parton model kTpQCD\_v2.0 [4, 5] which embedded generalized parton distribution functions (PDFs). All model details are extensively discussed in the literature and we focus only on the updated results for pseudorapidity distributions, nuclear modification factor,  $R_{p\text{Pb}}(\eta, p_T, b) = dn_{p\text{Pb}}/(N_{\text{coll}}(b)dn_{pp})$  and the pseudorapidity asymmetry,  $Y_{\text{asym}}^h(p_T) = R_{p\text{Pb}}^h(p_T, \eta < 0)/R_{p\text{Pb}}^h(p_T, \eta > 0)$ . These predictions are testable with a short 5.02A TeV run ( $10^6$  events).

## II. NUCLEAR SHADOWING AND JET QUENCHING AT LHC ENERGIES

Monte Carlo models as HIJING1.0 [6], HIJING2.0 [7] and HIJING/B $\bar{\text{B}}$ 2.0 [1–3] have been developed to study hadron productions in  $p + p$ ,  $p + A$  and  $A + A$  collisions. They are essentially two-component models, which describe the production of hard parton jets and the soft interaction between nucleon remnants. The hard jets production is calculated employing collinear factorized multiple minijet within pQCD. A cut-off scale  $p_0$  in the transverse momentum of the final jet production has to be introduced below which ( $p_T < p_0$ ) the interaction is considered nonperturbative and is characterized by a finite soft parton cross section  $\sigma_{\text{soft}}$ . Jet cross sections depend on the parton distribution functions (PDFs) that are parametrized from a global fit to data [7, 8].

Nucleons remnants interact via soft gluon exchanges described by the string models [9, 10] and constrained from lower energy  $e + e$ ,  $e + p$ ,  $p + p$  data. The produced hard jet pairs and the two excited remnants are treated as independent strings, which fragments to resonances that decay to final hadrons. Longitudinal beam jet string fragmentations strongly depend on the values used for string tensions that control quark-anti-quark ( $q\bar{q}$ ) and diquark-anti-diquark ( $qq\bar{q}\bar{q}$ ) pair creation rates and strangeness suppression factors ( $\gamma_s$ ). In the HIJING1.0 and HIJING2.0 models a constant (vacuum value) for the effective value of string tension is used,  $\kappa_0 = 1.0$  GeV/fm. At high initial energy density the novel nuclear physics is due to the possibility of multiple longitudinal flux tube overlapping leading to strong longitudinal color field (SCF) effects. Strong Color Field (SCF) effects are modeled in HIJING/B $\bar{\text{B}}$ 2.0

by varying the effective string tensions value. SCF also modify the fragmentation processes resulting in an increase of (strange)baryons which play an important role in the description of the baryon/meson anomaly. In order to describe  $p+p$  and central Pb + Pb collisions data at the LHC we have shown that an energy and mass dependence of the mean value of the string tension should be taken into account [3]. Moreover, to better describe the baryon/meson anomaly seen in data a specific implementation of  $J\bar{J}$  loops, has to be introduced. For a detailed discussion see Refs. [2, 3]. Similar results can be obtained by including extra diquark-antidiquark pair production channels from strong coherent fields formed in heavy-ion collisions [11].

All HIJING type models implement nuclear effects such as nuclear modification of the partons distribution functions, i.e., *shadowing* and *jet quenching* via a medium induced parton splitting process (collisional energy loss is neglected) [6]. In the HIJING1.0 and HIJING/B $\bar{B}$ 2.0 models Duke-Owen (DO) parametrization of PDFs [12] is used to calculate the jet production cross section with  $p_T > p_0$ . In both models using a constant cut-off  $p_0 = 2 \text{ GeV}/c$  and a soft parton cross section  $\sigma_{soft} = 54 \text{ mb}$  fit the experimental  $p+p$  data. However, for  $A+A$  collisions in HIJING/B $\bar{B}$ 2.0 model we introduced an energy and mass dependence of the cut-off parameter,  $p_0(s, A)$  [2, 3] at RHIC and at the LHC energies, in order not to violate the geometrical limit for the total number of minijets per unit transverse area.

In HIJING2.0 [7] model that is also a modified version of HIJING1.0 [6] the Gluck-Reya-Vogt (GRV) parametrization of PDFs [13] is implemented. The gluon distributions in this different parametrization are much higher than the DO parametrization at small  $x$ . In addition, an energy-dependent cut-off  $p_0(s)$  and  $\sigma_{soft}(s)$  are also assumed in order to better describe the Pb + Pb collisions data at the LHC.

One of the main uncertainty in calculating charged particle multiplicity density in Pb + Pb collisions is the nuclear modification of parton distribution functions, especially gluon distributions at small  $x$ . In HIJING type models one assume that the parton distributions in a nucleus (with atomic number  $A$  and charge number  $Z$ ),  $f_{a/A}(x, Q^2)$ , are factorizable into parton distributions in a nucleon ( $f_{a/N}$ ) and the parton(a) shadowing factor ( $S_{a/A}$ ),

$$f_{a/A}(x, Q^2) = S_{a/A}(x, Q^2) A f_{a/N}(x, Q^2) \quad (1)$$

In our calculations we will assume that the shadowing effect for gluons and quarks is the

same, and neglect also the QCD evolution ( $Q^2$  of the shadowing effect). At this stage, the experimental data unfortunately can not fully determine the  $A$  dependence of the shadowing. We will follow the  $A$  dependence as proposed in Ref.[6] and use the following parametrization,

$$\begin{aligned}
S_{a/A}(x) &\equiv \frac{f_{a/A}(x)}{A f_{a/N}(x)} \\
&= 1 + 1.19 \log^{1/6} A [x^3 - 1.2x^2 + 0.21x] \\
&\quad - s_a (A^{1/3} - 1) \left[ 1 - \frac{10.8}{\log(A+1)} \sqrt{x} \right] e^{-x^2/0.01}, \tag{2}
\end{aligned}$$

$$s_a = 0.1, \tag{3}$$

The term proportional to  $s_a$  in Eq. 2 determines the shadowing for  $x < x_0$ , (where  $x_0=0.1$ ) with the most important nuclear dependence, while the rest gives the overall nuclear effect on the structure function in  $x > x_0$  with some very slow  $A$  dependence. This parametrization can fit the overall nuclear effect on the quark structure function in the small and medium  $x$  region [6]. Because the remaining of Eq. 2 has a very slow  $A$  dependence, we will only consider the impact parameter dependence of  $s_a$ . After all, most of the jet productions occur in the small  $x$  region where shadowing is important:

$$s_a(b) = s_a \frac{5}{3} (1 - b^2/R_A^2), \tag{4}$$

where  $R_A$  is the radius of the nucleus, and  $s_a = s_q = s_g = 0.1$ . The LHC data [3] indicate that such quark(gluon) shadowing is required to fit the centrality dependence of the central charged particle multiplicity density in Pb + Pb collisions. This constrain on quark(gluon) shadowing is indirect and model dependent. Therefore, it is important to study directly quark(gluon) shadowing in  $p + A$  collisions at the LHC. In contrast, in HIJING2.0 [7],[8], a different  $A$  parametrization ( $(A^{1/3} - 1)^{0.6}$ ) and much stronger impact parameter dependence of the gluon ( $s_g = 0.22 - 0.23$ ) and quark ( $s_q = 0.1$ ) shadowing factor is used in order to fit the LHC data. Due to this stronger gluon shadowing the jet quenching effect has to be neglected [7].

Note, all HIJING type models assume a scale-independent form of shadowing parametrization (fixed  $Q^2$ ). This approximation could breakdown at very large scale due to dominance of gluon emission dictated by the DGLAP [14] evolution equation. At  $Q = 2.0$  and  $4.3$  GeV/ $c$ , which are typical scales for mini-jet production at RHIC and LHC respectively, it was shown that the gluon shadowing varies by approximately 13% in EPS09 parametrizations [15].

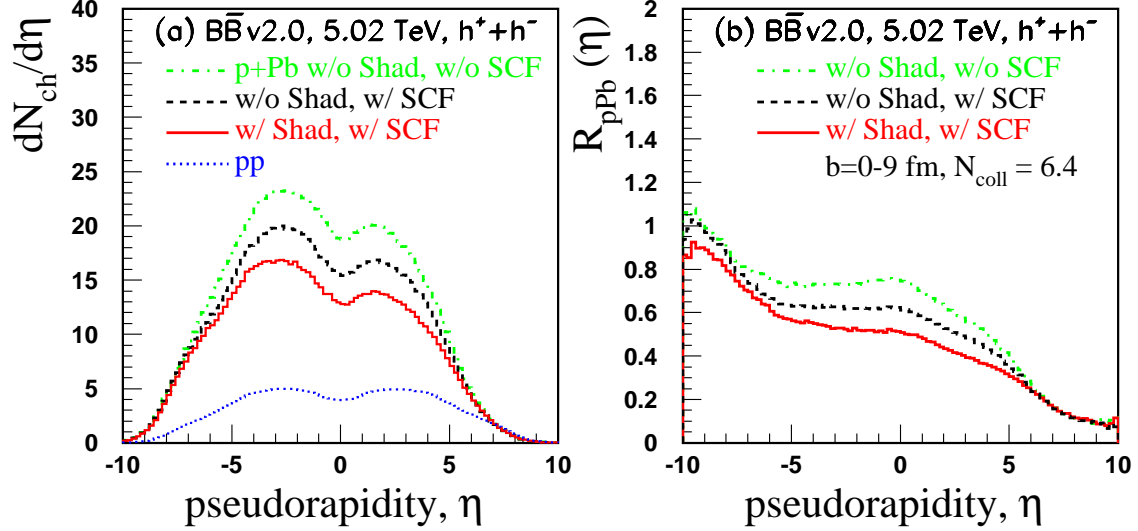


FIG. 1: (Color online) (a) HIJING/ $\bar{B}\bar{B}$ 2.0 predictions of charged particles pseudorapidity distribution ( $dN_{\text{ch}}/d\eta$ ) for minimum bias (MB)  $p+\text{Pb}$  collisions at 5.02A TeV. Solid curves includes fixed  $Q^2$  shadowing functions from HIJING1.0 [6] and SCF effects, while the dashed curve has SCF effects but no shadowing. The dotdashed curve are the results without SCF and Shadowing. (b) Ratio  $R_{p\text{Pb}}(\eta)$  calculated assuming  $N_{\text{coll}}(\text{MB}) = 6.4$

### III. HIJING/ $\bar{B}\bar{B}$ PREDICTIONS

Figure 1 shows HIJING/ $\bar{B}\bar{B}$ 2.0 predictions of the global observables  $dN_{\text{ch}}/d\eta$  and  $R_{p\text{Pb}}(\eta) = (dN_{p\text{Pb}}^{\text{ch}}/d\eta)/(N_{\text{coll}}dN_{pp}^{\text{ch}}/d\eta)$  characteristics of minimum bias  $p + \text{Pb}$  collisions at 5.02A TeV. The predictions for  $p + p$  are also shown. Minijet cutoff and string tension parameters  $p_0 = 3.1 \text{ GeV}/c$  and  $\kappa = 2.0 \text{ GeV}/\text{fm}$  for  $p + \text{Pb}$  are determined from fits to  $p + p$  and  $A + A$  systematics from RHIC to the LHC (see Refs. [2, 3], for details). Note, these calculations assume no *jet quenching*.

The absolute normalization of  $dN_{\text{ch}}/d\eta$  is however sensitive to the low  $p_T \lesssim 2 \text{ GeV}/c$  nonperturbative hadronization dynamics that is performed via LUND [9] string JETSET [10] fragmentation as constrained from lower energy  $e+e$ ,  $e+p$ ,  $p+p$  data. The default HIJING1.0 parametrization of the fixed  $Q_0^2 = 2 \text{ GeV}^2$  shadow function leads to substantial reduction (solid histograms) of the global multiplicity at the LHC. It is important to emphasize that the no shadowing results (dashed curves) are substantially reduced in HIJING/ $\bar{B}\bar{B}$ 2.0 relative to no shadowing prediction with default HIJING/1.0 from Ref. [6], because both the default

minijet cut-off  $p_0 = 2 \text{ GeV}/c$  and the default vacuum string tension  $\kappa_0 = 1 \text{ GeV}/\text{fm}$  (used in HIJING1.0) are generalized to vary monotonically with centre of mass (cm) energy per nucleon  $\sqrt{s}$  and atomic number,  $A$ . As discussed in [2, 3] systematics of  $p + p$  and Pb+Pb multiparticle production from RHIC to the LHC are used to fix the energy ( $\sqrt{s}$ ) and the  $A$  dependence to a cut-off parameter  $p_0(s, A) = 0.416 \sqrt{s}^{0.191} A^{0.128} \text{ GeV}/c$  and a mean value of the string tension  $\kappa(s, A) = \kappa_0 (s/s_0)^{0.04} A^{0.167} \text{ GeV}/\text{fm}$  [2]. The above formulae lead to  $p_0 = 3.1 \text{ GeV}/c$  and  $\kappa = 2.1 \text{ GeV}/\text{fm}$  at  $5.02A \text{ TeV}$  for  $p + \text{Pb}$  collisions. For  $p + p$  collisions at  $5.02 \text{ TeV}$  we use a constant cut-off parameter  $p_{0pp} = 2 \text{ GeV}/c$  and a string tension value of  $\kappa_{pp} = 1.9 \text{ GeV}/\text{fm}$ .

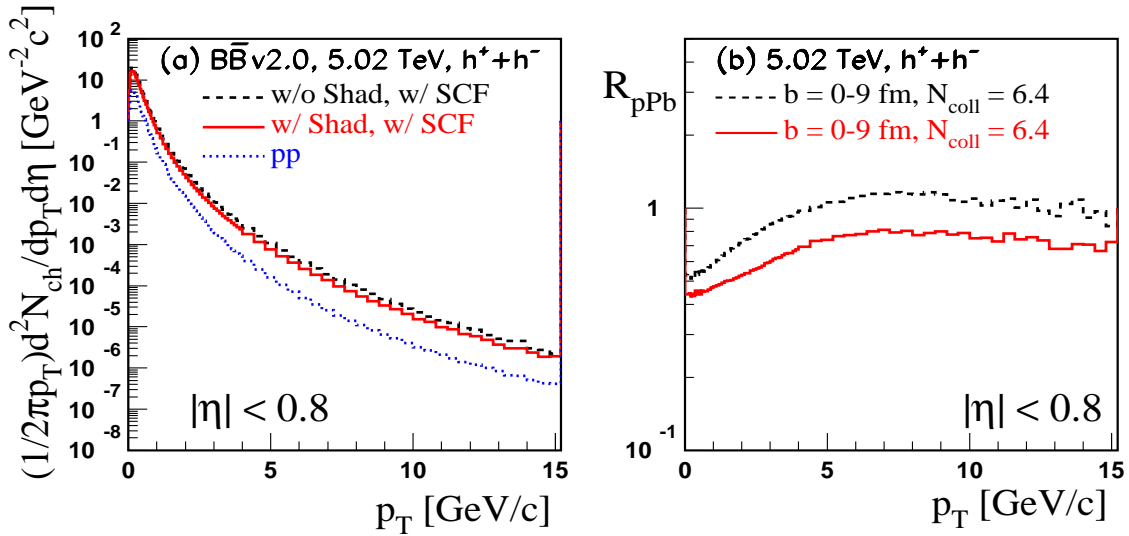


FIG. 2: (Color online) (a) Minimum bias transverse momentum distributions at mid-pseudorapidity  $|\eta| < 0.8$  predicted by HIJING/B $\bar{\text{B}}$ 2.0 with (solid histogram) and without (dashed histogram) HIJING1.0 shadowing functions [6]. The results for  $p + p$  collisions at  $5.02 \text{ TeV}$  (dotted histogram) are also included. (b) The mid-pseudorapidity nuclear modification factor of charged hadrons  $R_{p\text{Pb}}$  from HIJING/B $\bar{\text{B}}$ 2.0 model. The solid and dashed histograms have the same meaning as in part (a).

Note, even in the case of no shadowing shown in Fig. 1, the increase to  $p_0 = 3.1 \text{ GeV}/c$  from  $p_0 = 2 \text{ GeV}/c$  (value used in  $p + p$  at  $5.02 \text{ TeV}$ ) causes a significant reduction by a factor of roughly two of the minijet cross section and hence final pion multiplicity. This reduction of minijet production is also required to fit the low charged particle multiplicity growth in  $A + A$  collisions from RHIC to LHC (a factor of 2.2) [16].

We interpret this as additional phenomenological evidence for gluon saturation physics not encoded in leading twist shadow functions. The  $p_T > 5$  GeV/ $c$  minijets tails are unaffected but the bulk low  $p_T < 5$  GeV/ $c$  multiplicity distribution is sensitive to this extra energy ( $\sqrt{s}$ ) and  $A$  dependence of the minijet shower suppression effect. It is difficult to relate  $p_0$  to saturation scale  $Q_{sat}$  directly, because in HIJING hadronization proceeds through longitudinal field string fragmentation. The energy ( $\sqrt{s}$ ) and  $A$  dependence of the string tension value arises from strong color field (color rope) effects not considered in CGC phenomenology that assumes  $k_T$  factorized gluon fusion hadronization. HIJING hadronization of minijets is not via independent fragmentation functions as in PYTHIA [10], but via string fragmentation with gluon minijets represented as kinks in the strings. The interplay between longitudinal string fragmentation dynamics and minijets is a nonperturbative feature of HIJING type models. The approximate triangular (or trapezoidal) rapidity asymmetry seen in the ratio  $R_{pPb}(\eta)$  sloping downwards from the nuclear beam fragmentation region at negative pseudorapidity  $\eta < -5$  toward  $1/N_{coll}$  in the proton fragmentation region ( $\eta > 5$ ) is a basic Glauber geometric effect first explained in Refs. [17, 18] and realized via string fragmentation in HIJING.

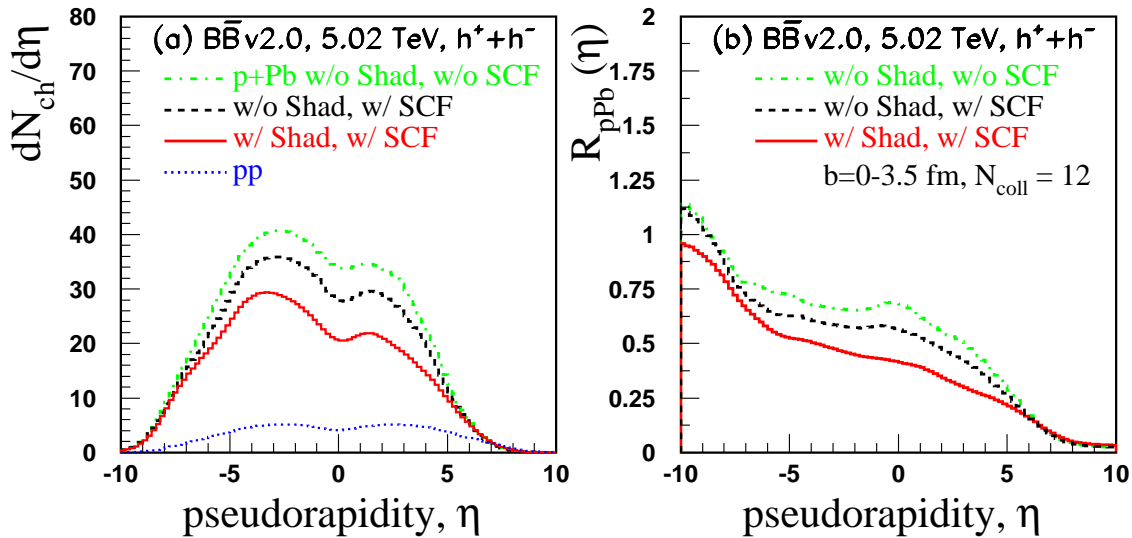


FIG. 3: (Color online) (a) HIJING/BB2.0 predictions of charged particles pseudorapidity distribution ( $dN_{ch}/d\eta$ ) for central 0-20%  $p$ +Pb collisions at 5.02A TeV. The solid, dashed and the dotted histograms have the same meaning as in Fig. 1.

In Fig. 2 are displayed the predicted transverse spectra and nuclear modification factor

for charged hadrons at mid-pseudorapidity,  $|\eta| < 0.8$ . Including shadowing and SCF effects reduces  $R_{pPb}$  from unity to about 0.7 in the interesting 5 to 10 GeV/c region close to the prediction of Color Glass Condensate model (KKT04) [19]. A similar nuclear modification factor is found [20] using leading order (LO) pQCD collinear factorization with HIJING2.0 parameterization of shadowing functions [8], GRV parton distribution functions (nPDF) from Ref. [13], and hadron fragmentation functions from Ref. [21].

Figure 3 and Fig. 4 show HIJING/B $\bar{B}$ 2.0 predictions of the global observables  $dN_{ch}/d\eta$  and  $R_{pPb}(\eta) = (dN_{pPb}^{ch}/d\eta)/(N_{coll}dN_{pp}^{ch}/d\eta)$  characteristics of central (0-20 %)  $p + Pb$  collisions at 5.02A TeV. The number of binary collisions  $N_{coll} \approx 12$ . Figure 3 and Fig. 4 The results are similar with those presented in Fig. 1 and Fig. 2. In a scenario with SCF and shadowing effects the  $R_{pPb}(p_T)$  are slightly lower than in MB event selection. In contrast in a scenario with SCF effects and without shadowing the model predicts no suppression for high  $p_T > 5$  GeV/c charged particles ( *i.e.*,  $\approx 1$ ).

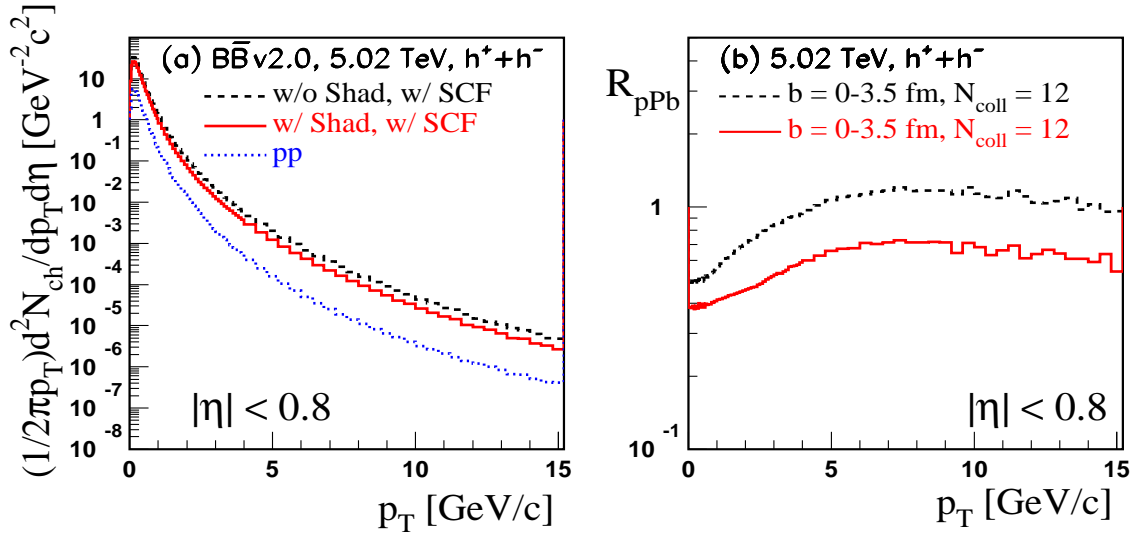


FIG. 4: (Color online) (a) Minimum bias transverse momentum distributions at mid-pseudorapidity  $|\eta| < 0.8$  (Fig. 4a) and nuclear modification factor for central 0-20 %  $p + Pb$  collisions at 5.02 ATeV predicted by HIJING/B $\bar{B}$ 2.0 model. The solid and dashed histograms have the same meaning as in Fig. 2.



#### IV. CALCULATIONS WITH $k_T$ pQCD\_v2.0 MODEL

The kTpQCD\_v2.0 code is based on a phenomenologically enhanced, perturbative QCD improved parton model described in details in Refs. [4, 5]. The main feature of this model is the phenomenologically generalized parton distribution function in order to deal with the non-perturbative effects at relatively low- $x$  (i.e. small  $p_T$ ) values. The model includes the so called intrinsic- $k_T$  parameter as phenomenological corrections for non-perturbative effects determined by data from wide energy range of nucleon-nucleon (mainly  $pp$ ) collisions. Moreover, within the framework of this model, the broadening of the intrinsic- $k_T$  in proton-nucleus ( $pA$ ) or nucleus-nucleus ( $AA$ ) collisions is related to the nuclear multiple scattering. This can generate enhancement of the nuclear modification factor, the so called Cronin effect [22, 23], which appears within the  $3 \text{ GeV}/c \leq p_T \leq 9 \text{ GeV}/c$  region from SPS to RHIC energies.

The kTpQCD\_v2.0 code calculates the invariant cross section for hadron production in  $pp$ ,  $pA$  or  $AA$  collisions, which can be described at LO or NLO levels in the  $k_T$ -enhanced pQCD-improved parton model on the basis of the factorization theorem. The code provides Monte Carlo based integration of the convolution [5]:

$$\begin{aligned}
 E_h \frac{d\sigma_h^{pp}}{d^3p_T} &= \frac{1}{S} \sum_{abc} \int_{VW/z_c}^{1-(1-V)/z_c} \frac{dv}{v(1-v)} \int_{VW/vz_c}^1 \frac{dw}{w} \int^1 dz_c \\
 &\times \int d^2\mathbf{k}_{Ta} \int d^2\mathbf{k}_{Tb} f_{a/p}(x_a, \mathbf{k}_{Ta}, Q^2) f_{b/p}(x_b, \mathbf{k}_{Tb}, Q^2) \\
 &\times \left[ \frac{d\tilde{\sigma}}{dv} \delta(1-w) + \frac{\alpha_s(Q_R)}{\pi} K_{ab,c}(s, v, w, Q, Q_R, Q_F) \right] \frac{D_c^h(z_c, Q_F^2)}{\pi z_c^2}, \quad (5)
 \end{aligned}$$

where we introduced the 3-dimensional generalized parton distribution functions in a factorized form,

$$f(x, \mathbf{k}_T, Q^2) = f(x, Q^2) \cdot g(\mathbf{k}_T). \quad (6)$$

Here, the function  $f(x, Q^2)$  represents the standard 1-dimensional LO or NLO PDF as a function of momentum fraction of the incoming parton  $x$  at factorization scale  $Q$ ,  $d\tilde{\sigma}/dv$  represents the Born cross section of the partonic subprocess  $ab \rightarrow cd$ ,  $K_{ab,c}(s, v, w, Q, Q_R, Q_F)$  is the corresponding higher order correction term, and the LO or NLO fragmentation function (FF),  $D_c^h(z_c, Q_F^2)$ , gives the probability for parton  $c$  to fragment into a hadron,  $h$  with momentum fraction  $z_c$  at fragmentation scale  $Q_F$ . We use the conventional proton level

( $S, V, W$ ) and parton level ( $s, v, w$ ) kinematical variables of next-to-leading order calculations (for more details see Refs. [5, 24, 25]).

In this analysis we consider fixed scales: the factorization and the renormalization scales are connected to the momentum of the intermediate jet,  $Q = Q_R = \kappa \cdot p_q$  (where  $p_q = p_T/z_c$ ), while the fragmentation scale is connected to the final hadron momentum,  $Q_F = \kappa \cdot p_T$ . The value of  $\kappa = 2/3$ .

We introduce the phenomenologically generalized 3-dimensional (3-D) PDF which is assumed to be factorized to a standard PDF (at its  $Q$  scale) and a 2-D initial transverse-momentum distribution,  $g(\mathbf{k}_T)$  of partons containing its 'intrinsic- $k_T$ ' parameter as in Refs. [4, 5, 26, 27]. We demonstrated the success of such a treatment at LO level in Ref. [4], and a  $K_{jet}$ -based NLO calculations in Refs. [28, 29]. In our phenomenological approach the transverse-momentum distribution is described by a Gaussian,

$$g(\mathbf{k}_T) = \frac{1}{\pi \langle k_T^2 \rangle} e^{-k_T^2 / \langle k_T^2 \rangle} \quad (7)$$

Here,  $\langle k_T^2 \rangle$  is the 2-D width of the  $k_T$  distribution and it is related to the magnitude of the average transverse momentum of a parton as  $\langle k_T^2 \rangle = 4 \langle k_T \rangle^2 / \pi$ . In order to reproduce the nucleon-nucleon collisions at relatively low- $x$ , we assume  $\langle k_T^2 \rangle = 2.5 \text{ GeV}^2/c^2$ .

As a standard 1-D PDFs, MRST (at central gluon (cg)) [30] was used in eq. (6). For FF we use the most recent parameterizations KKP from Ref. [31]. These sets of PDF and FF can be applied down to very small scales ( $Q^2 \approx 1.25 \text{ GeV}^2$ ). Therefore, we can perform calculations at relatively small transverse momenta,  $p_T \geq 2 \text{ GeV}$  for our fixed scales.

### A. Initial State Nuclear Effects in $pA$ and $AA$ Collisions

Proton-nucleus and nucleus-nucleus collisions can be described by including collision geometry, saturation in nucleon-nucleon ( $NN$ ) collision number, and shadowing inside the nucleus. In the framework of Glauber picture, the cross section of hadron production in nucleus-nucleus collision can be written as an integral over impact parameter,  $b$ :

$$E_h \frac{d\sigma_h^{AA'}}{d^3p_T} = \int d^2b d^2r t_A(r) t_{A'}(|\mathbf{b} - \mathbf{r}|) \cdot E_\pi \frac{d\sigma_\pi^{pp}(\langle k_T^2 \rangle_{pA}, \langle k_T^2 \rangle_{pA'})}{d^3p}, \quad (8)$$

where  $pp$  cross section on the right hand side represents the cross section from eq. (5), but with an increased widths compared to the original transverse-momentum distributions (7)

in  $pp$  collisions, as a consequence of nuclear multiscattering (see eq. (9)). Here  $t_A(b) = \int dz \rho_A(b, z)$  is the nuclear thickness function (in terms of the density distribution of nucleus  $A$ ,  $\rho_A$ ), normalized as  $\int d^2b t_A(b) = A$ . For the  $Pb$  nuclei Woods–Saxon formula was applied.

The initial state broadening of the incoming parton’s distribution function is accounted for by an increase in the width of the Gaussian parton transverse momentum distribution in eq. (7):

$$\langle k_T^2 \rangle_{pA} = \langle k_T^2 \rangle_{pp} + C \cdot h_{pA}(b) \quad (9)$$

Here,  $\langle k_T^2 \rangle_{pp}$  is the width of the transverse momentum distribution of partons in  $pp$  collisions,  $h_{pA}(b)$  describes the number of *effective*  $NN$  collisions at impact parameter  $b$ , which impart an average transverse momentum squared  $C$ . The effectivity function  $h_{pA}(b)$  can be written in terms of the number of collisions suffered by the incoming proton in the target nucleus,  $\nu_A(b) = \sigma_{NN} t_A(b)$ , where  $\sigma_{NN}$  is the inelastic  $NN$  cross section:

$$h_{pA}(b) = \begin{cases} \nu_A(b) - 1 & \nu_A(b) < \nu_m \\ \nu_m - 1 & \text{otherwise} \end{cases} \quad (10)$$

We have found that for realistic nuclei the maximum number of semihard collisions is  $3 \leq \nu_m \leq 4$  with  $C = 0.4 \text{ GeV}^2/c^2$ .

Furthermore, the PDFs are modified in the nuclear environment by the ‘shadowing’ effect [8, 32–34]. This effect and isospin asymmetry are taken into account on average using a scale independent parameterization of the shadowing function  $S_{a/A}(x)$  adopted from Ref. [26]:

$$f_{a/A}^{(1)}(x, Q^2) = S_{a/A}(x) \left[ \frac{Z}{A} f_{a/p}(x, Q^2) + \left( 1 - \frac{Z}{A} \right) f_{a/n}(x, Q^2) \right], \quad (11)$$

where  $f_{a/n}(x, Q^2)$  is the standard 1-dimensional PDF for the neutron and  $Z$  is the number of protons. In the present work, we display results obtained with the EKS99 [32], EPS08 [33] and HKN [34] parameterization, and with the updated HIJING parameterization [8]. The former three has an anti-shadowing feature, while the latter one incorporates different quark and gluon shadowing, and has an impact-parameter dependent and an impact-parameter independent version. The impact-parameter dependence is taken into account by a term  $\propto (1 - b^2/R_A^2)$ , which re-weights the shadowing effect inside the nucleus.

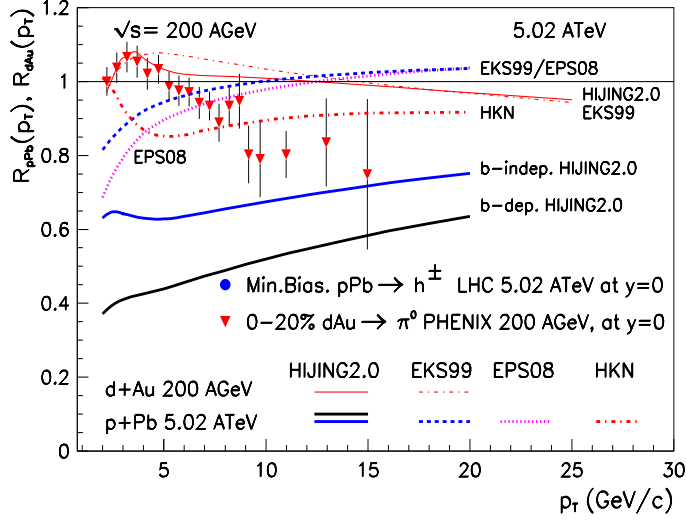


FIG. 5: (Color online) Predictions updated at 5.02A TeV from Ref. [1, 20] for central 0 – 20% ( $b < 3.5$  fm)  $pPb$  at midrapidity. Predictions with with DGLAP  $Q^2$  evolved HIJING[8], EKS99[32], EPS08[33], and HKN[34] shadowing are also shown. The data for  $d + Au$  collisions at 200 GeV are from PHENIX [38, 39]

## B. Results on Nuclear Effects

The nuclear modification factor,  $R_{pPb}^{h^\pm}(p_T)$  is presented on Fig 5 for charge-averaged hadrons, using various shadowing functions,  $S_{a/Pb}(x)$ . On this plot HIJING [8], EKS99 [32], EPS08 [33], and HKN [34] shadowing parameterizations are plotted. For the case of HIJING parameterization both impact-parameter dependent/independent versions are plotted. Calculations were made for  $\sqrt{s} = 5.02$  ATeV,  $|\eta| < 0.3$ , and 0 – 20% central  $pPb$ . Note, due to the lack of  $b$ -dependence of the above mentioned shadowing functions, this is equal to the minimum bias results as well. All details and parameters are the same as in Ref. [1]. See more details in Refs. [4, 35–37].

We perform calculations on rapidity asymmetry defined as:

$$Y_{asym}^h(p_T) = \frac{E_h d^3 \sigma_p^h Pb / d_T^p |_{\eta < 0}}{E_h d^3 \sigma_p^h Pb / d_T^p |_{\eta > 0}} = \frac{R_{pPb}^h(p_T, \eta < 0)}{R_{pPb}^h(p_T, \eta > 0)}. \quad (12)$$

For these calculations we used kT<sub>p</sub>QCD\_v2.0 with various type of shadowing functions.

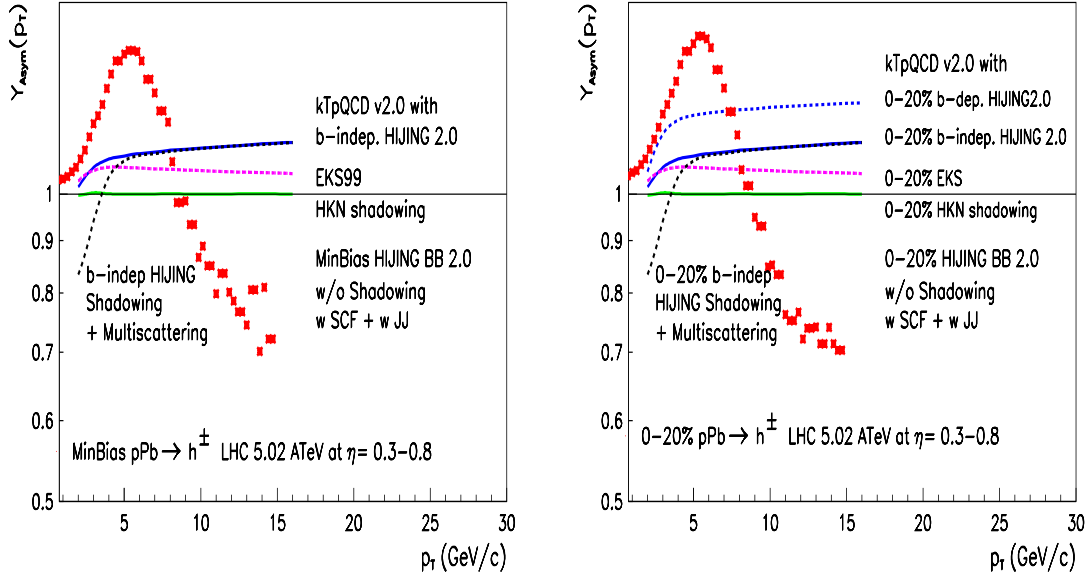


FIG. 6: (Color online) Predictions for  $Y_{asym}^h(p_T)$  updated at 5.02 ATeV from Refs. [1, 20] for MB events selection (left panel) and central 0 – 20%  $pPb$  collisions (right panel). Compared are fixed  $Q^2$  deeply shadowed HIJING predictions [8] with and without impact parameter dependence. Predictions with DGLAP  $Q^2$  evolved EKS99[32] EPS08[33] shadowing are shown. The results obtained using HIJING/ $B\bar{B}$  v2.0 model (stars) are also included.

Calculations are at  $\sqrt{s} = 5.02 ATeV$  using the  $0.3 < |\eta| < 0.8$  rapidity range to the backward and forward directions. Results are an extension of those published in Ref. [37] on effects close-to-midrapidity region. The results are plotted on Figure 6 for unidentified charged hadron production in minimum bias (MB)  $pPb$  collisions (*left panel*). One compare the calculations within kTpQCD\_v2.0 code including HIJING [8], EKS99 [32], EPS08 [33], HKN [34] shadowing parameterizations. The results using HIJING/ $B\bar{B}$  v2.0 model are obtained in a scenario without shadowing but including SCF and  $J\bar{J}$  loops effects [3]. Due to soft physics embedded in the model the predictions are different compared with pQCD inspired model kTpQCD\_v2.0. The reason for this is under study now and will be presented elsewhere. Similar results are plotted for central (0 – 20%)  $p+Pb$  collisions in the right panel.

## V. CONCLUSION

In conclusion, even with a small sample of  $10^6$  events the study of  $R_{p\text{Pb}}(p_T)$  or central relative to peripheral NMF ( $R_{\text{CP}}(p_T)$ ) could provide a definitive constraint on nuclear shadowing implemented within different pQCD inspired models and CGC saturation models, with high impact on the interpretation or reinterpretation of the bulk and hard probes for nucleus-nucleus (Pb+Pb) collisions at LHC energies.

## VI. ACKNOWLEDGMENTS

VTP and JB are supported by the Natural Sciences and Engineering Research Council of Canada. MG is supported by the Division of Nuclear Science, U.S. Department of Energy, under Contract No. DE-AC03-76SF00098 and DE-FG02-93ER-40764 (associated with the JET Topical Collaboration Project). GGB, GB, MG, and PL also thanks for the Hungarian grants OTKA PD73596, NK778816, NIH TET\_10-1\_2011-0061 and ZA-15/2009. GGB was partially supported by the János Bolyai Research Scholarship of the HAS. MP is supported by the Romanian Authority for Scientific Research, CNCS-UEFIS-CDI project number PN-II-ID-2011-3-0368.

- 
- [1] G. G. Barnaföldi, J. Barrette, M. Gyulassy, P. Levai and V. Topor Pop, Phys. Rev. C **85**, 024903 (2012).
  - [2] V. Topor Pop, M. Gyulassy, J. Barrette, C. Gale and A. Warburton, Phys. Rev. C **86**, 044902 (2012).
  - [3] V. Topor Pop, M. Gyulassy, J. Barrette, and C. Gale, Phys. Rev. C **84**, 022002 (2011); V. Topor Pop, M. Gyulassy, J. Barrette, C. Gale, and A. Warburton, Phys. Rev. C **83**, 024902 (2011).
  - [4] Y. Zhang, G. Fai, G. Papp, G.G. Barnaföldi, and P. Levai, Phys. Rev. **C65**, 034903 (2002).
  - [5] G. Papp, G.G. Barnaföldi, P. Levai, and G. Fai, hep-ph/0212249.
  - [6] X. -N. Wang, M. Gyulassy, Phys. Rev. Lett. **68**, 1480 (1992); *ibid.* Phys. Rev. D **44**, 3501 (1991).

- [7] W. -T. Deng, X. -N. Wang, and R. Xu, Phys. Rev. C **83**, 014915 (2011); Phys. Lett. **B701**, 133 (2011).
- [8] S. -Y. Li, X. -N. Wang, Phys. Lett. **B527**, 85 (2002).
- [9] B. Andersson, G. Gustafson, B. Nilsson-Almqvist, Nucl. Phys. **B281**, 289 (1987); B. Nilsson-Almqvist, E. Stenlund, Comput. Phys. Commun. **43**, 387 (1987).
- [10] H. -U. Bengtsson, T. Sjostrand, Comput. Phys. Commun. **46**, 43 (1987).
- [11] P. Levai, D. Berenyi, A. Pasztor, V. V. Skokov, J. Phys. G **38**, 124155 (2011).
- [12] D. W. Duke, J. F. Owens, Phys. Rev. D **30**, 49 (1984).
- [13] M. Gluck, E. Reya, A. Vogt, Z. Phys. **C67**, 433 (1995).
- [14] G. Altarelli and G. Parisi, Nucl. Phys. **B126**, 298 (1977).
- [15] K. J. Eskola, H. Paukkunen, and C. A. Salgado, JHEP **0904**, 065 (2009).
- [16] J. W. Harris [ALICE Collaboration], AIP Conf. Proc. **1422**, 15 (2012).
- [17] S. J. Brodsky, J. F. Gunion, J. H. Kuhn, Phys. Rev. Lett. **39**, 1120 (1977).
- [18] A. Adil, M. Gyulassy, Phys. Rev. C **72**, 034907 (2005).
- [19] D. Kharzeev, Y. V. Kovchegov, K. Tuchin, Phys. Rev. D **68**, 094013 (2003).
- [20] P. Levai, Nucl. Phys. **A862-863**, 146 (2011); G. G. Barnafoldi, G. Fai, P. Levai, B. A. Cole and G. Papp, Indian J. Phys. **84**, 1721 (2010).
- [21] B. A. Kniehl, G. Kramer, B. Potter, Nucl. Phys. **B582**, 514 (2000).
- [22] J.W. Cronin *et al.* (CP Collaboration), Phys. Rev. **D11**, 3105 (1975).
- [23] D. Antreasyan *et al.* (CP Collaboration), Phys. Rev. **D19**, 764 (1979).
- [24] F. Aversa, P. Chiappetta, M. Greco, and J.Ph. Guillet, Nucl. Phys. **B327**, 105 (1989).
- [25] P. Aurenche *et al.*, Eur. Phys. J. **C9**, 107 (1999);  
P. Aurenche, *et al.* Eur. Phys. J. **C13**, 347 (2001).
- [26] X.N. Wang, Phys. Rev. **C61**, 064910 (2001).
- [27] C.Y. Wong and H. Wang, Phys. Rev. **C58**, 376 (1998).
- [28] G.G. Barnaföldi, P. Lévai, G. Papp, G. Fai, and Y. Zhang, APH NS Heavy Ion Phys. **18** (2003).
- [29] G.G. Barnaföldi, P. Lévai, G. Papp, G. Fai, and Y. Zhang,  
Proc. of ISMD '02, World Sci. (2003).
- [30] A.D. Martin, R.G. Roberts, W.J. Stirling, and R.S. Thorne, Eur. Phys. J. **C23**, 73 (2002).
- [31] B.A. Kniehl, G. Kramer and B. Pötter, Nucl. Phys. **B597**, 337 (2001).

- [32] K.J. Eskola, V.J. Kolhinen and C.A. Salgado, Eur. Phys. J. **C9**, 61 (1999).
- [33] K. J. Eskola, H. Paukkunen, and C. A. Salgado, JHEP **0807**, 102 (2008).
- [34] M. Hirai, S. Kumano and M. Miyama, Phys. Rev. **D64**, 034003 (2001).
- [35] G. G. Barnafoldi, G. Fai, P. Levai, B. A. Cole and G. Papp, Indian J. Phys. **84**, 1721 (2010).
- [36] B. A. Cole, G. G. Barnafoldi, P. Levai, G. Papp and G. Fai, arXiv:hep-ph/0702101.
- [37] A. Adeluyi, G. G. Barnafoldi, G. Fai and P. Levai, Phys. Rev. C **80**, 014903 (2009).
- [38] S. S. Adler *et al.* [PHENIX Collaboration], Phys. Rev. Lett. **91**, 072303 (2003).
- [39] S. S. Adler *et al.* (PHENIX Collaboration), Phys. Rev. Lett. **98**, 172302 (2007).